Ultrasonic Range Measurements on the Human Body

D. Weenk[1,2], B.J.F. van Beijnum[1,2], A. Droog[1], H.J. Hermens[1,2,3], P.H. Veltink[1]
[1]MIRA Institute for Biomedical Technology and Technical Medicine, University of Twente, Enschede, the Netherlands
[2]CTIT Centre for Telematics and Information Technology, University of Twente, Enschede, the Netherlands
[3]Roessingh Research and Development, Enschede, the Netherlands
d.weenk@utwente.nl

Abstract—**Ambulatory range estimation on the human body is important for the assessment of the performance of upper- and lower limb tasks outside a laboratory. In this paper an ultrasound sensor for estimating ranges on the human body is presented and validated during gait. The distance between the feet is estimated based on the time of flight and compared to an optical reference. The signal to noise ratio of the received signal is used as a measure for the uncertainty of the range estimate. For example when rejecting distance estimates with a signal to noise ratio smaller than 5, the mean absolute distance difference between the ultrasound sensor and an optical reference system is 7.0 mm (sd 7.1 mm) over six walking trials.**

Keywords—ultrasound, time of flight, range, human body, gait

I. INTRODUCTION

On-body range measurements are important for assessing the performance of upper- and lower limb tasks [1], [2]. Traditionally, force plates in combination with optical systems are used for this. These systems calculate 3D positions of several markers on the body. Disadvantage of these systems is that measurements are restricted to a lab with cameras, which limits the capture area to a few walking cycles. Ambulatory systems, using for instance inertial sensors, are becoming increasingly popular for tracking human movement. Measurements can be performed outside a lab and even at home, without restrictions in measurement volume, allowing the measurement of different daily-life activities. However, with inertial sensors, relative positions of body segments cannot be measured directly, but are estimated from segment orientations in combination with their lengths [3]. This leads to errors when segment lengths are incorrectly measured or estimated.

Roetenberg et al. [4] investigated a portable magnetic position and orientation tracker, with promising results. By using a 3D magnetic source, positioned on the back of the body, and 3D magnetic sensors placed at different body segments, the accuracy was approximately 8 mm in position and 5º in orientation during movement. Disadvantage is the relatively large size and weight (21 cm diameter, 11 cm height, 450 g), making it unsuitable for placing it on a foot.

Schepers et al. [5] used shoes instrumented with force/moment and inertial sensors for the ambulatory assessment of foot placement during walking. Lateral foot placement and stride length were estimated from integration of inertial sensor signals (angular velocities and accelerations). However, this method leads to large position errors (drift) after integration. Besides, only position changes are calculated and since the begin positions are unknown this does not result in relative positions of the feet.

Huitema et al. [6] described an ultrasonic motion analysis system, capable of measuring important human gait parameters. Two small ultrasonic receivers were attached to both shoes, while a transmitter was placed stationary on the floor. By subtracting the positions of the feet with zero velocity, step and stride lengths were estimated. Disadvantage is the transmitter placed on the floor, limiting the maximum measurement distance to 8.6 m.

In this paper the design and validation of an ambulatory ultrasonic on-body range measurement-system is described. We selected ultrasound transducers because they are small and light-weight, making them suitable for placing them on several human body segments. In addition they are low cost and not affected by ferromagnetic materials (especially in floor when walking), as is the case when using magnetic position estimation.

II. DESIGN OF THE SENSOR

The ultrasound sensor is based on estimating the time of flight (t_{ToF}). This is in our case the time it takes for an ultrasound signal to travel from a transmitter to a receiver. When this time is known, it can be multiplied with the speed of sound (v_s) to get the distance,

$$d_{ultrasound} = v_s \cdot t_{ToF}. \tag{1}$$

The speed of sound is temperature dependent and in air the expression is

$$v_s = 331.4 \cdot (1 + 1.83 \cdot 10^{-3} \cdot T_C), \tag{2}$$

with T_C the temperature in ºC [7].

In the remainder of this Section the estimation of the time of flight is described, from the signal processing to the used hardware.

A. Time of flight estimation

A typical example of a received and amplified ultrasound signal is shown in Fig. 1 (top), the center frequency of the signal is 40 kHz.

The authors would like to thank PIDON, the Dutch ministry of economic affairs and the Provinces Overijssel and Gelderland for financially supporting the Fusion project.

The signal strength has a negative correlation with the time of flight and is therefore estimated by calculating the root-mean-square (RMS), after removing the offset. Recorded noise at the beginning of the signal, which is not related to the transmitted pulse, is eliminated (Fig. 1) by overwriting these samples with the mean of the signal. For signals with large RMS, nothing is eliminated, to be able to detect small time of flights as well.

To filter out noise – for example, picked up in the circuit between the receiver and the microcontroller – the recorded signal is band-pass filtered using an 8th order zero-phase Butterworth filter with cut-off frequencies 35 and 45 kHz. The amplifier is tuned to be able to pick up also weak signals when the transducers are approximately 90 cm apart. This leads to a clipping signal when the transducers are close together, causing the slope of the envelope to be steeper than normal (larger frequency than 40 kHz). Therefore, we make an exception to the band-pass filter when this occurs. When the transducers are close together, which is estimated using the RMS, only a high-pass filter is applied.

To be able to accurately estimate the start of the received pulse (Fig. 1, top), and thus the time of flight, the filtered signal is normalized and its envelope is calculated by rectifying and low-pass filtering (10 kHz, 4th order zero-phase Butterworth filter), see Fig. 1 (bottom).

Subsequently, the time of flight (t_{ToF}) is estimated from the envelope using two successive thresholds, A and B (Fig. 1, bottom). Multiplying by the speed of sound (v_s) this gives a first estimate of the range, see (1). This range is re-calibrated using a calibration board, as will be described later.

B. Hardware

The schematic of the sensor is shown in Fig. 2. The central part of this ultrasonic range measurement system is an ATmega328P microcontroller running at 14.7456 MHz. The processor will output one pulse of a certain width to the gate of the FET (F1), and during that (short) time a current will flow through the primary windings of the transformer (T1), this will induce a high voltage at the secondary side that will excite the transmit transducer (400ST120). Due to its mechanical and electrical properties in combination with the frequency tuned transformer, the transducer will output several in amplitude drastically diminishing pulses (40 kHz). As soon as the pulse to the transformer has been generated, the controller starts converting and storing the signal coming from the amplifier. For this purpose the processor is using a 10 bits Analog to Digital Converter, sampling at 195 kHz, of which only the HI byte is used to save on time and storage. For storage512 bytes are used, which is sufficient to measure a range up to ±90 cm. The receive transducer (400SR120) is excited by the acoustic signal sent from the transmitter. The amplifier consists mainly of an LM386 low voltage audio power amplifier. Potentiometer P1 is used for setting the sensitivity while P2 is used for scaling the output signal of the amplifier (powered from 5 V) to the input of the Analog to Digital Converter in the

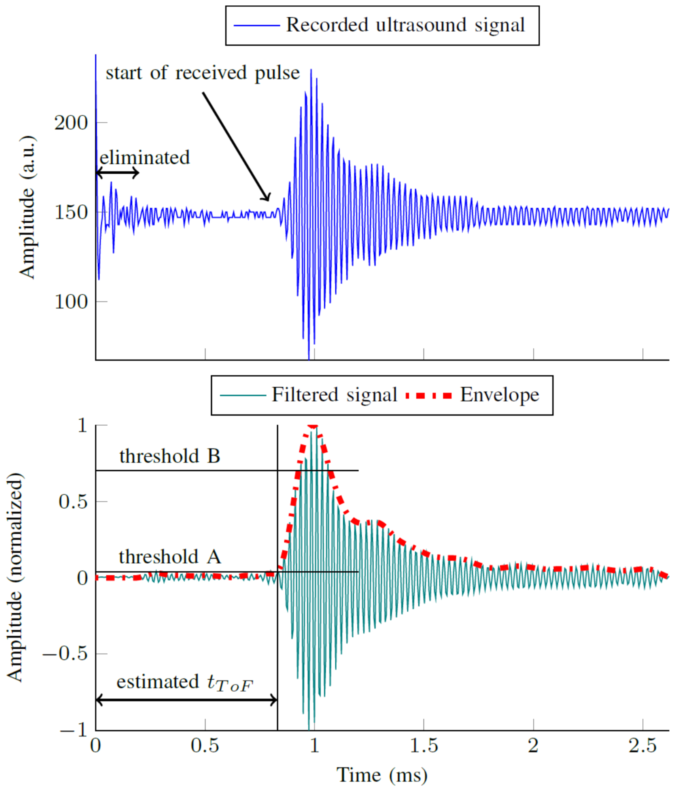

Figure 1. Typical example of a recorded ultrasound signal (top). After eliminating the first samples (that are not related to the sent pulse), the signal is bandpass filtered and normalized and the envelope is calculated (bottom). From the envelope the time of of flight is estimated using two successive thresholds (A and B).

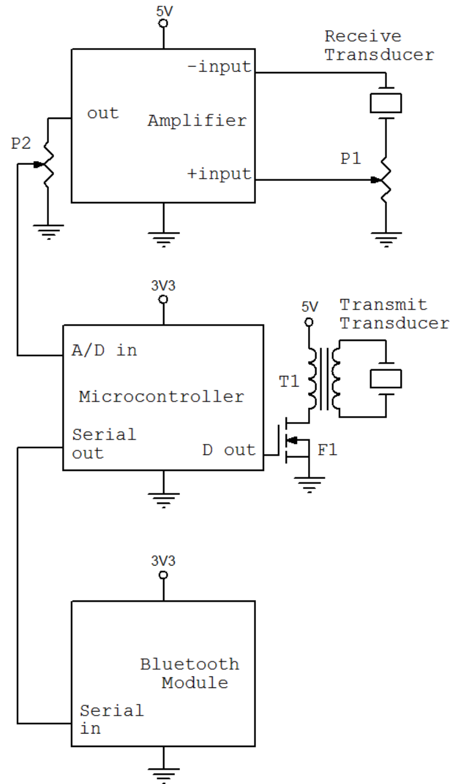

Figure 2. Schematic of the ultrasound sensor. The transmit transducer including transformer is placed on one foot, while the receive transducer and the amplifier are placed on the other foot, see Fig. 4. The microcontroller and bluetooth module are placed at the waist of the subject.

ATmega328P microcontroller (powered from 3.3 V). When 512 samples have been taken, these samples are sent via a Bluetooth connection to a computer where the distance is calculated using MATLAB®. The Bluetooth module is powered by 3.3 V and is directly controlled by the microcontroller with a baud rate of 230k4 bits per second. After the 512 bytes of data is sent to the computer, the controller starts over again with generating the pulse to the gate of the FET. This occurs approximately 13.3 times per second.

III. VALIDATION METHODS

To validate the ultrasound sensor, the estimated distance was compared to an optical reference system.

A. Set-up

The Xsens ForceShoes (Xsens Technologies B.V. [8]), containing two 6D force/moment sensors and two inertial sensors, were used (Fig. 3). On one shoe we mounted the transmitting transducer, on the other shoe the receiving transducer. Both transducers were placed in the sole of the forefoot in front of the inertial sensor (Fig. 4). The microcontroller and Bluetooth module were placed at the waist of the subject.

Six walking trials of two healthy volunteers were recorded.

B. Reference measurement

For a reference measurement, three reflective markers were placed at each forefoot as in Fig. 4. Their trajectories were recorded using six Vicon® cameras. From the three markers, orientation matrices – describing the orientation of right ($\boldsymbol{R}^{gr}$) and left ($\boldsymbol{R}^{gl}$) forefoot with respect to the Vicon-global frame (ψ_g) – were constructed using cross products of the vectors connecting these markers. This was necessary to transform the vectors pointing from the toe markers to the ultrasound transducers ($\boldsymbol{p}^r_{us,r}$ and $\boldsymbol{p}^l_{us,l}$, in right and left shoe frame, ψ_r and ψ_l respectively) to frame ψ_g [9]. The reference distance measurement, d_{ref}, was then calculated

$$d_{ref} = ||\boldsymbol{p}^g_{rtoe} + \boldsymbol{R}^{gr}\boldsymbol{p}^r_{us,r} - (\boldsymbol{p}^g_{ltoe} + \boldsymbol{R}^{gl}\boldsymbol{p}^l_{us,l})||_2. \quad (3)$$

Subsequently this distance was compared to the distance estimated with the ultrasound sensor system ($d_{ultrasound}$).

Figure 3. Xsens ForceShoe (Xsens Technologies B.V. [8]), containing two 6D force/moment sensors and two inertial sensors. The ultrasound transducers were mounted near the inertial sensor in the forefoot, indicated with the arrow.

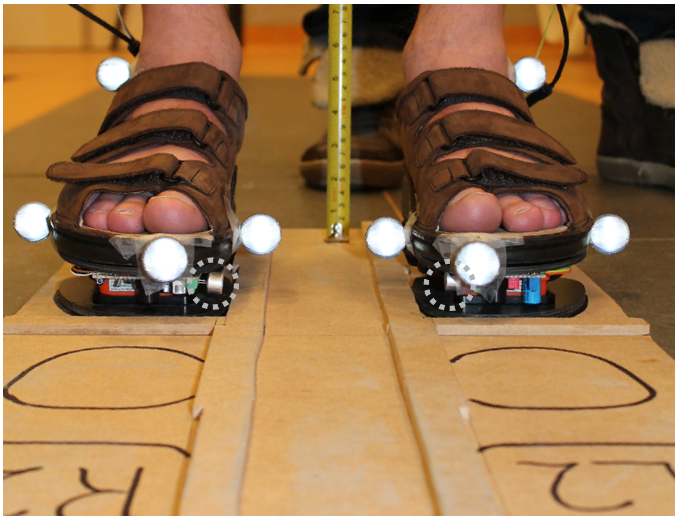

Figure 4. Measurement set-up for for validating the ultrasound range measurements. The subject wearing the Xsens ForceShoes is standing on the calibration board. The ultrasound transducers were placed in the sole next to the inertial sensor in the front part (forefoot) of the ForceShoe, indicated with the dashed grey circles. For the reference measurement three reflective markers were placed on the forefoot segment of each ForceShoe. The ankle-markers were not used in this study.

C. Calibration

A calibration-board (Fig. 5) was developed to calibrate for speed of sound, which is temperature dependent (2), and for inaccuracies caused by the threshold method used for estimating the time of flight. On the board, each foot was placed on three different locations, similar to standing normally (e.g. L1-R1) and walking with different step lengths (e.g. L1-R2). From these positions the distance between the ultrasound transducers was measured using a tape measure (d_{ruler}). Based on the RMS of the ultrasound signal, two calibration regions were defined with two different offsets and gains. One region where the signal was not clipping, for RMS values below a threshold, and a region where the RMS exceeded that threshold and the amplified signal was clipping, as described in Section II-A. For each set of measurements (in this case two) new calibration measurements were performed, to calibrate the distance estimates (a constant temperature was assumed during a set of measurements).

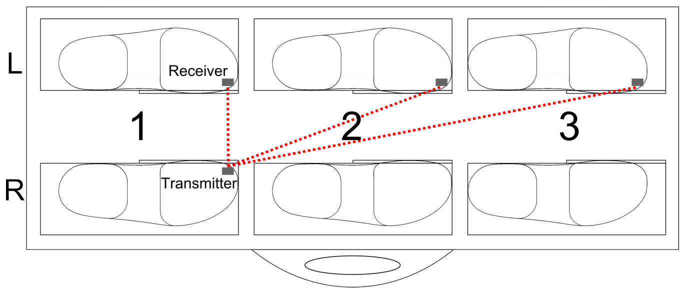

Figure 5. Calibration board used for calibrating the distance estimates. The distance between the transmitter and receiver was measured with a tape measure, after which calibration parameters were calculated. On the board, each foot can be placed on three different locations, similar to standing normally (e.g. R1-L1) and walking with different step lengths (e.g. R1-L2 or R1-L3). During al these combinations there is line of sight between transmitter and receiver, as indicated by the red dashed lines.

D. Synchronizing reference measurement and ultrasound sensor

To be able to compare both range estimates, it is important that they are synchronized in time. For this purpose, the cross correlation was calculated. The time for which the correlation was maximal was used to synchronize both ranges. Subsequently, the reference range estimates were resampled to match the range estimates from the ultrasound sensor, after which they were subtracted and the absolute value was taken,

$$d_{abs,diff} = |d_{ref} - d_{ultrasound}|. \tag{4}$$

IV. VALIDATION RESULTS

A. Calibration measurements

The mean and standard deviations of the calibration measurements are listed in Table I. Because the sensor system is not symmetric (one shoe contains a transmitter, the other a receiver) and because of inaccuracy of measuring the distance with the tape measure, calibration parameters are obtained from a combination of these measurements, causing the difference between d_{ruler} and $d_{ultrasound}$. As can be seen in Table I, the standard deviation from the R3-L1 measurements is relatively large. Therefore we calculate the signal-to-noise ratio (SNR) by estimating the mean power from two frequency regions; 40±3 kHz and the remaining frequencies. The mean SNR for the R1-L1 measurement is 80 and for the R3-L1 it is 19. The relation between the SNR and the distance estimates is investigated in more detail in the next Section.

B. Walking trials

The absolute distance difference versus the SNR from all six walking trials is plotted in Fig. 6. As expected, the SNR is small when the absolute distance difference ($d_{abs,diff}$) is large. This allows us to use the SNR as a measure for accepting or rejecting the ultrasound range estimates. For example, rejecting all estimates with an SNR less or equal to 5 shifts the mean of $d_{abs,diff}$ from 110.7 to 7.0 mm (standard deviation from 203.7 to 7.1). When choosing the SNR threshold 20, the mean absolute difference is 5.8 mm with a standard deviation of 5.0. It should be noted that 52% of the distance estimates are rejected in this case, see Fig. 7.

TABLE I. OVERVIEW OF CALIBRATION MEASUREMENTS. d_{ruler} IS THE DISTANCE MEASURED WITH A TAPE MEASURE. FROM THE ESTIMATED DISTANCE WITH THE ULTRASOUND SENSOR, $d_{ultrasound}$, THE MEAN AND STANDARD DEVIATION (SD) ARE SHOWN. RESULTS ARE FROM ONE MEASUREMENT, FOR EACH CALIBRATION POSITION ABOUT 20 SECONDS.

Calibration	d_{ruler} (mm)	$d_{ultrasound}$ (mm)	
		mean	sd
R1-L1	137	137.0	0.1
R1-L2	373	375.1	1.2
R1-L3	683	680.3	2.5
R3-L3	137	137.6	0.1
R3-L2	351	349.1	0.9
R3-L1	688	690.6	4.6

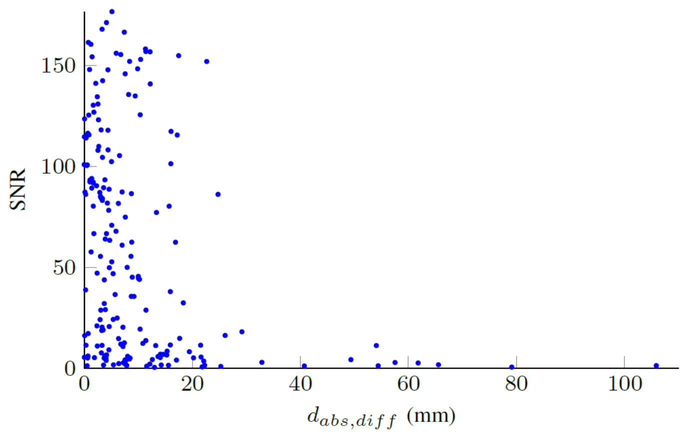

Figure 6. The absolute distance difference ($d_{abs,diff}$) versus the SNR from all six walking trials. The *x*-axis is limited for displaying purposes. Absolute differences of up to approximately 700 mm were observed, however, only for SNR values smaller than 5.

The comparison of the ultrasonic range estimates with the reference measurements for one walking trial is shown in Fig. 8. The estimates when setting the SNR threshold to 5 are also shown, rejecting 35% of the range estimates from all trials. The mean absolute difference for this trial is 6.7 mm (sd 5.3). For this SNR threshold, the distance differences over all trials are plotted versus the reference distance in Fig. 9.

V. DISCUSSION

For SNR thresholds larger than 20, the mean of the absolute distance difference stays between 5 and 6 mm (Fig. 7). SNR thresholds below 5 result in a mean absolute difference of 11.2 (sd 39.3) mm or more. Therefore, it is recommended to set the SNR threshold between 5 and 20. When setting the threshold to 20, 52% of the range estimates are rejected. This leaves approximately 7 distance estimates per second on average, which can be very useful for example for position estimation in a fusion algorithm together with inertial sensors with a higher sample rate. This sensor fusion is currently being investigated using methods from [10]. In applications where more range estimates are required, the SNR threshold should be set lower.

When the distance between the transducers increases, the SNR becomes smaller (Section IV-A). When looking at the maximum distance that is measured by the sensor over all walking trials (Fig. 7, bottom), we see that when setting the SNR threshold to 8 or larger, distances larger than 700 mm are no longer detected. If this is important for the application, the SNR threshold should be set smaller than 8.

It should be noted that the presented validation is a comparison with an optical system. Next to the errors of the positions of the optical system itself – which can be up to several millimeters [11] – there are errors introduced in measuring the distances between the transducers on the calibration board and the positions of the markers on the shoes with respect to the transducers. The calibration parameters obtained for example using L1-R2 and L1-R3 are different from the ones obtained using L3-R2 and L3-R1. This is why calibration parameters were obtained from a combination of all these measurements, which can cause errors. Once information about the walking cycle is available (that is, which foot is in

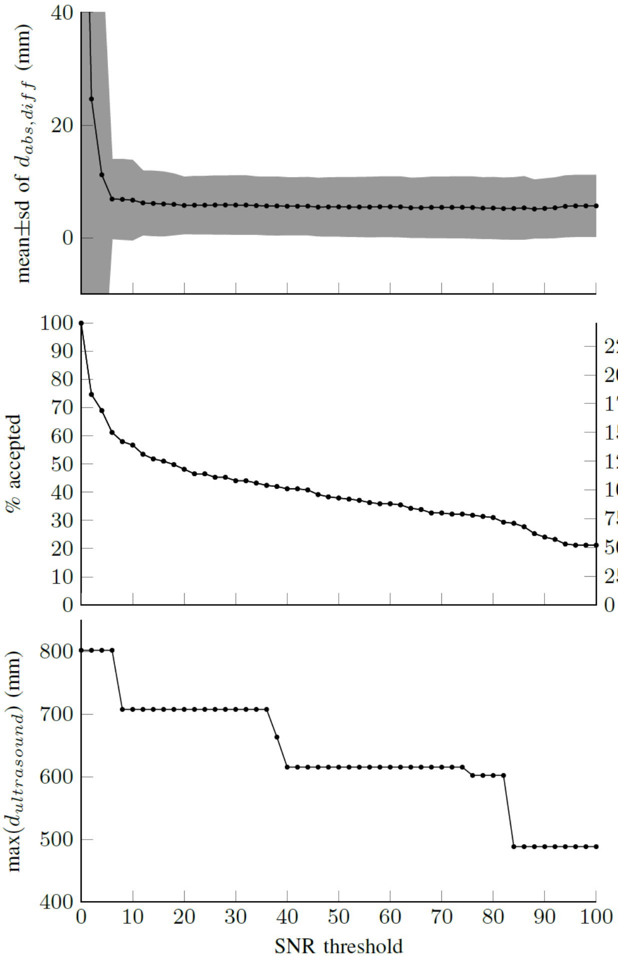

Figure 7. Top: the mean (±sd, shaded) of $d_{abs,diff}$ as a function of the SNR threshold for all walking trials (245 distance estimates). For display purposes the y-axis is limited; when no SNR threshold is set (SNR threshold=0), the mean absolute difference is 110.7 (sd 203.7) mm. Middle: the percentage (number (N) on right y-axis) of the estimates that are accepted for each value of the SNR threshold. Bottom: the maximum distance that is estimated during the walking trials, for each threshold. It can be seen that for SNR threshold larger than 40, distances larger than ±600 mm are no longer detected.

front of the other), the calibration parameters corresponding to this can be used, to improve the accuracy. This information is available when adding information from inertial sensors.

When looking at the distance estimates in Fig. 8, we see approximately 5 steps of the walking trial, which is the limit of the optical reference system. From the figure the distance between the feet during double stance can be seen when looking at the maxima. The minima indicate the distance between the feet during midstance or midswing, i.e. the swinging foot passes the stance foot [12]. Alternating times between peaks or alternating heights of the peaks can be an indication of an asymmetric walking pattern.

In this study the ultrasound sensor was validated for measuring foot distance during gait. Our expectation is that, considering reflections from the floor, the performance of the sensor when used on other parts of the human body – for example, on trunk and hand for estimating maximum reach –

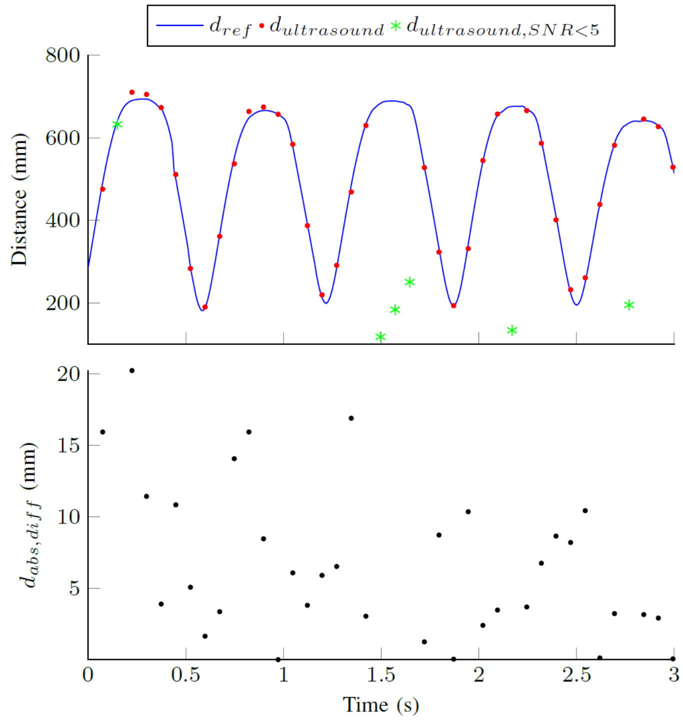

Figure 8. The reference distance (d_{ref}) and the distances estimated with the ultrasound sensor ($d_{ultrasound}$) for one walking trial (top). Setting the SNR threshold to 5 results in the red estimates (the green estimates are rejected). The absolute difference is shown in the bottom figure (mean 6.7, sd 5.3 mm).

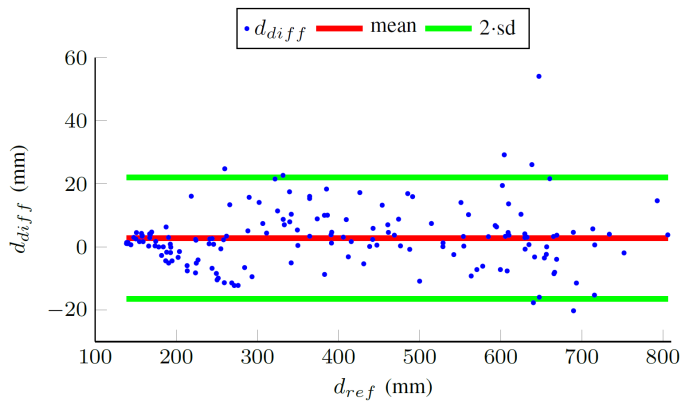

Figure 9. The difference between the distance estimated with the ultrasound sensor and the reference distance (d_{diff}) versus the reference distance (d_{ref}) for all walking trials when using an SNR threshold of 5. The mean (2.6 mm) and two times the standard deviation (sd, 9.6 mm) are indicated by the horizontal lines.

will be similar. There should however be a direct line of sight between transmitter and receiver.

We validated the sensor using the ForceShoes of which the influence on gait appeared to be small [13]. The sensor can however be used of course on other shoes as well.

An offset is observed in the difference between the distance estimates, see Fig 9. This can be explained because the time of flight is more often underestimated than overestimated, as can also be seen in Fig. 8 (top). In Fig. 9 we also see that the distance difference is relatively small when feet are close together. For example, for reference distances smaller than 200 mm the mean absolute distance difference is 2.5 mm (sd 1.7 mm) over all walking trials. In Fig. 10 the relative difference versus the reference distance is shown.

No significant correlation between velocity estimated with the reference system and $d_{abs,diff}$ was found.

Disadvantage of the presented sensor is the amplifier, which is clipping when the feet are close together, causing the slope of the envelope to be steeper than normal. This problem is however solved by introducing two calibration regions; when the received signal is or is not clipping, estimated using the RMS of the received signal. Another solution could be to use a different amplifier, for example a time-gain-compensation amplifier which amplifies more when the time of flight becomes larger [14]. Another disadvantage are the required cables from microcontroller to both transducers, causing the microcontroller and Bluetooth module to be placed at the waist of the subject. This was necessary for time synchronization, that is, the microcontroller starts recording at the moment a pulse was sent to the transmitter. This could however be implemented wireless, given a suitable protocol (accuracy of maximally a few microseconds is needed [15] to keep the error below 1 mm) is used. For the current calibration method it is assumed that the temperature stays constant during a set of measurements. If the temperature would change however during measurements – for example, when walking out of a heated room – this would immediately lead to an error in the estimated distance. A rule of thumb is that for a 10 ºC change in temperature, the speed of sound and hence the estimated distance, changes with approximately 2% (see (2) and [7]). To overcome this problem a temperature sensor could be added to the system, provided that the body temperature is not influencing this sensor.

The time of flight is currently estimated using MATLAB®. It is also possible to do this on a microcontroller and sending only the range estimates (and corresponding SNR) to the PC.

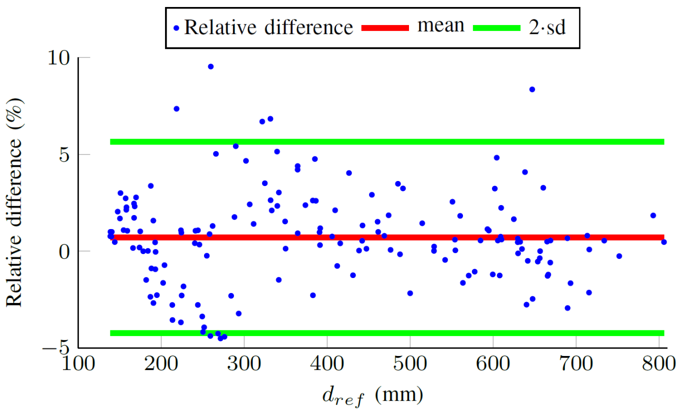

Figure 10. The relative difference (in %) versus the reference distance (d_{ref}) for all walking trials when using an SNR threshold of 5. The mean (0.7) and two times the standard deviation (sd, 2.5) are indicated by the horizontal lines.

VI. CONCLUSION AND FUTURE WORK

An ultrasound sensor for estimating ranges on the human body is presented and validated using an optical reference system during gait. The SNR can be used as a measure for the uncertainty of a distance estimate. When rejecting all distance estimates with an SNR smaller than 5, the mean absolute distance difference between ultrasound sensor and reference system is 7.0 mm (sd 7.1 mm) over six walking trials. In this case 35% of the estimates are rejected. In future work we will fuse the range measurements with inertial sensors for 3D estimation of (relative) positions of the feet.

ACKNOWLEDGMENT

The authors would like to thank M. van der Coelen, A.A.G. Geessink, F.J. van der Hoek and B. Verstoep, for investigating the possibilities regarding range measurements between the feet.

REFERENCES

[1] C. M. Said, P. A. Goldie, A. E. Patla, E. Culham, W. A. Sparrow, and M. E. Morris, "Balance during obstacle crossing following stroke," Gait & Posture, vol. 27, no. 1, pp. 23 – 30, 2008.

[2] C. M. Dean and R. B. Shepherd, "Task-related training improves performance of seated reaching tasks after stroke. a randomized controlled trial," Stroke, vol. 28, no. 4, pp. 722–728, 1997.

[3] D. Roetenberg, H. Luinge, and P. Slycke, "Xsens MVN: full 6DOF human motion tracking using miniature inertial sensors," Xsens Motion Technologies BV, Tech. Rep, 2009.

[4] D. Roetenberg, P. Slycke, A. Ventevogel, and P. Veltink, "A portable magnetic position and orientation tracker," Sensors and Actuators A: Physical, vol. 135, no. 2, pp. 426 – 432, 2007.

[5] H. M. Schepers, E. H. Van Asseldonk, C. Baten, and P. H. Veltink, "Ambulatory estimation of foot placement during walking using inertial sensors," Journal of biomechanics, vol. 43, no. 16, pp. 3138–3143, 2010.

[6] R. B. Huitema, A. L. Hof, and K. Postema, "Ultrasonic motion analysis system - measurement of temporal and spatial gait parameters," Journal of biomechanics, vol. 35, no. 6, pp. 837–842, 2002.

[7] P. P. L. Regtien, F. Van Der Heijden, M. J. Korsten, and W. Olthuis, Measurement science for engineers. Kogan Page Science, 2004.

[8] "The Xsens Technologies B.V. website," 2013, July 31. [Online].Available: http://www.xsens.com

[9] J. B. Kuipers, Quaternions and Rotation Sequences: A Primer with Applications to Orbits, Aerospace, and Virtual Reality. Princeton University Press, 2002.

[10] F. Gustafsson, Statistical sensor fusion, 1st ed. Studentlitteratur, 2010.

[11] Y. Ehara, H. Fujimoto, S. Miyazaki, M. Mochimaru, S. Tanaka, and S. Yamamoto, "Comparison of the performance of 3d camera systems II," Gait & Posture, vol. 5, no. 3, pp. 251 – 255, 1997. [Online].

[12] C. L. Vaughan, B. L. Davis, and J. C. O'connor, Dynamics of human gait. Human Kinetics Publishers USA, 1992.

[13] H. Schepers, "Ambulatory assessment of human body kinematics and kinetics," Ph.D. dissertation, University of Twente, 2009.

[14] Z. Yu and G. C. M. Meijer, "A programmable time-gain-compensation (TGC) amplifier for medical ultrasonic echo signal processing," in Solid-State and Integrated-Circuit Technology, 2008. ICSICT 2008. 9th International Conference on. IEEE, 2008, pp. 1725–1728.

[15] S. M. Lasassmeh and J. M. Conrad, "Time synchronization in wireless sensor networks: a survey," in IEEE SoutheastCon 2010 (SoutheastCon), Proceedings of the. IEEE, 2010, pp. 242–245.